Picosecond Kerr-gated time-resolved resonance Raman spectroscopy of the [Ru(phen)(2)dppz](2+) interaction with DNA

ARTICLE *in* JOURNAL OF INORGANIC BIOCHEMISTRY · AUGUST 2002

Impact Factor: 3.44 · DOI: 10.1016/S0162-0134(02)00466-X · Source: PubMed

7 AUTHORS, INCLUDING:

Björn Önfelt
KTH Royal Institute of Technology
62 PUBLICATIONS **2,010** CITATIONS
SEE PROFILE

Bengt Nordén
Chalmers University of Technology
511 PUBLICATIONS **17,558** CITATIONS
SEE PROFILE

Pavel Matousek
Science and Technology Facilities Council
346 PUBLICATIONS **7,118** CITATIONS
SEE PROFILE

Eimer M Tuite
Newcastle University
43 PUBLICATIONS **1,939** CITATIONS
SEE PROFILE

ELSEVIER

Journal of Inorganic Biochemistry 91 (2002) 286–297

Journal of Inorganic Biochemistry

www.elsevier.com/locate/jinorgbio

Picosecond Kerr-gated time-resolved resonance Raman spectroscopy of the $[Ru(phen)_2dppz]^{2+}$ interaction with DNA

Johan Olofsson[b], Björn Önfelt[b], Per Lincoln[b], Bengt Nordén[b], Pavel Matousek[c], Anthony W. Parker[c], Eimer Tuite[a,*]

[a]*Department of Chemistry, Bedson Building, University of Newcastle, Newcastle-upon-Tyne NE1 7RU, UK*
[b]*Department of Physical Chemistry, Chalmers University of Technology, SE-412 96 Göteborg, Sweden*
[c]*Central Laser Facility, CLRC Rutherford Appleton Laboratory, Chilton, Didcot, Oxfordshire, OX11 OQX, UK*

Received 10 September 2001; received in revised form 1 May 2002; accepted 2 May 2002

Abstract

To investigate the basis of the 'light-switch' effect, the solvent dependence of the Kerr-gated picosecond-time resolved resonance Raman (TR^3) spectra of $[Ru(bpy)_2dppz]^{2+}$, $[Ru(phen)_2dppz]^{2+}$, and the modified complex $[Ru(phen)_2cpdppzOMe]^{2+}$ and a dimer $[\mu\text{-C4(cpdppz)}_2\text{-(phen)}_4Ru_2]^{4+}$ were studied. The investigation focussed on comparing the behaviour of $[Ru(phen)_2dppz]^{2+}$ in acetonitrile, ethanol, H_2O, D_2O, and DNA. The data are consistent with a model wherein excitation induces metal-to-ligand charge transfer (MLCT) to any of the ligands (termed the 'precursor' state) which, by interligand electron transfer (ILET), produces an excited state localised on the dppz ligand, $MLCT^1$. In water this state relaxes with a characteristic time of ~6 ps to a non-emissive state ($MLCT^2$). The TR^3 spectra in water, acetonitrile and DNA are all distinctly different. However, the early (4 ps) water spectrum resembles the spectrum in DNA. This interesting observation suggests that the DNA-bound excited state of the complex can be thought of as a model for the initial, poorly solvated state in water.

Keywords: Time resolved resonance Raman (TR^3) spectroscopy; Ruthenium; Dipyridophenazine; DNA; Metal-to-ligand charge transfer (MLCT)

1. Introduction

The interaction of substitution-inert metal complexes with DNA has generated considerable interest with respect to the development of DNA conformational probes, artificial nucleases, hybridization sensors, and anti-cancer drugs [1]. More than any other compound, complexes with the dipyrido[3,2-a:2′,3′-c]phenazine (dppz) ligand have attracted intense scrutiny because of their environmentally-sensitive photophysics [2–8]. $[Ru(phen)_2dppz]^{2+}$ (**1**; phen, phenanthroline) is a fluorescent probe for DNA since it luminesces moderately in the presence of dsDNA (ϕ~ 0.02) while displaying no detectable background emission in water, termed the 'light-switch' effect [9]. When bound to DNA by intercalation of the dppz ligand [10], the emission of $[Ru(phen)_2dppz]^{2+}$ is complex and multi-exponential with lifetimes of hundreds of nanoseconds [10,11]. The emission properties, including spectral maxima, bandwidths and especially lifetimes, are very sensitive to the enantiomer used and the DNA base sequence [12], although the origin of this variation is not yet fully understood.

Early steady-state luminescence studies [2,3,13] suggested that H-bonding or protonation at the phenazine nitrogens could be responsible for the quenching by water although it was noted that results in long-chain alcohols were not consistent with this proposal [3]. It has been demonstrated that excited state $[Ru(phen)_2dppz]^{2+}$ can be quenched by proton transfer [14]. However, recent time-resolved studies on fast timescales have indicated that more subtle processes involving two close-lying excited states may be responsible [15,16]. This concurs with findings that the luminescence lifetime and quantum yield of $[Ru(phen)_2dppz]^{2+}$ correlates better with solvent polarity than with H-bonding ability [4].

Accumulated evidence from absorption, luminescence, transient absorption, electrochemical and transient resonance Raman (TR^2) studies indicates that the lowest excited state in all media is localised on the dppz ligand

*Corresponding author. Tel.: +44-191-222-5523; fax: +44-191-222-6929.
E-mail address: e.m.tuite@ncl.ac.uk (E. Tuite).

0162-0134/02/$ – see front matter
PII: S0162-0134(02)00466-X

[2,3,13,17–20]. TR^2 studies have identified features that are characteristic of the different proposed states determining, for example, that a band at 1526 cm^{-1} is a marker for the state that emits in DNA and organic solvents [20]. MO calculations [18,21] have suggested that the two close-lying states may be localised within different regions of the ligand, with $MLCT^1$ localised on the phenanthroline part and $MLCT^2$ localised on the phenazine part. Recent TR^2 studies with deuterated complexes have enabled regional assignment of dppz vibrations as modes localised either on the phenanthroline or phenazine areas of dppz or delocalised in character [22].

Recently, the effect of environment on the photophysics of this complex has been investigated on faster time-scales to investigate the origin of the light-switch effect [15,16]. Picosecond transient absorption and time-resolved emission studies [15] found that in water an initially populated state (termed $MLCT^1$) [1] emitting at λ_{max} ~610 nm decayed rapidly (3 ps) to a second state ($MLCT^2$) emitting very weakly at λ_{max} ~800 nm from which efficient non-radiative decay (250 ps) to the ground state occurred. The absorption of $MLCT^2$ was considerably blue-shifted compared to $MLCT^1$. No such kinetics were observed for the complex in acetonitrile or bound to DNA where the emitting $MLCT^1$ state was instantaneously observed (<300 fs), and it was proposed that in both these media $MLCT^2$ was too high in energy to be populated: hence, the complex decayed to the ground state from $MLCT^1$ via radiative decay on the nanosecond timescale with features typical of MLCT states of ruthenium(II)polypyridyl complexes. It was suggested that in alcohols, $MLCT^2$ might be close in energy to $MLCT^1$ and could be thermally populated to provide a pathway for rapid non-radiative decay, although radiative decay from $MLCT^1$ at ~610 nm dominates the emission spectrum. More recently [16], ps-transient absorption and anisotropy studies have revealed that the fast decay is better described as a biexponential (0.7 and 4 ps), the first of these processes being accompanied by a large anisotropy change but not the second. It was suggested that the 0.7 ps decay was related to large-scale charge redistribution in the complex (perhaps from the phen to dppz ligand) and that the 4 ps process is solvation. These lifetimes are very similar to those reported for water reorganisation [23], suggesting that changes in electron distribution in the excited state may be connected with solvent reorganisation. It was also found that when bound to DNA the transient absorption of the complex evolved with lifetimes of 7 and 37 ps, with small accompanying changes in anisotropy, which was suggested to reflect the timescale of reorientation of the DNA basepairs about the intercalated excited state molecule.

Although previous time-resolved luminescence, transient absorption, and transient anisotropy studies have revealed the kinetics of the processes involved in the light-switch effect, they provide little information about the excited states involved. Our goal was to investigate the nature of the excited states that we have identified in ps-transient absorption and anisotropy studies, by employing the technique of picosecond time-resolved resonance Raman (TR^3) spectroscopy on the same timescale. Preliminary findings on $[Ru(bpy)_2dppz](BF_4)_2$ using an earlier version of the same experimental system have been reported [24] and were made possible by the development of an optical Kerr gate [25] that allowed TR^3 measurements in the presence of a fluorescent background and at single wavelengths with the Kerr gate suppressing Raman signals originating from the pump. The current studies expand on the previous findings by investigating a variety of different probe wavelengths and by looking for the first time at the TR^3 characteristics when the complex is bound to DNA. Moreover, we have investigated three related complexes, two monomers and a dimer (**1**–**3**), to correlate our TR^3 results with those previously obtained using transient absorption and anisotropy [16]. Ultimately we anticipate that the structural information accessible by TR^3 spectroscopy will prove invaluable in understanding the influence of environment on the photophysics of $[Ru(phen)_2dppz]^{2+}$.

2. Experimental

2.1. Materials

Literature methods were used for the preparation of racemic and enantiomeric $[Ru(phen)_2dppz]Cl_2$ [10] $[Ru(phen)_2cpdppzOMe]Cl_2$ and $[\mu$-C4(cpdppz)$_2$-(phen)$_4$-Ru$_2$]Cl$_4$ [26,27] (Fig. 1). Deionised water or solvents of the highest grade available were used. General chemicals were from Aldrich or Merck. All picosecond TR^3 measurements were made on complex solutions which were ~1 mM except for certain samples containing DNA where the complex concentration was ~0.5 mM as stated in the text. DNA concentration is expressed in terms of bases and was determined by absorption spectroscopy using $\epsilon_{260\ nm}$ = 6600 M^{-1} cm^{-1}. Calf thymus DNA from Sigma was dissolved in a buffer 5 mM sodium phosphate (pH 6.9)/100 mM NaCl to a concentration of ~15 mM and sonicated on ice with an ultrasonic probe using 2 s on/2 s off pulses for a total of 8 min. The sonicated DNA was then centrifuged at ~700×g for 20 min, and finally passed through a Whatman Hepa-vent filter to remove aggregated material. Comparison of the mobility of the sonicated DNA with a molecular weight ladder on a 1% agarose gel, revealed a polydisperse sample of ~100–1000-bp length. Sonication substantially reduced the viscosity and the sonicated DNA was suitable for use in the jet at concentrations of up to ~10 mM bases.

[1] $MLCT^1$ is equivalent to MLCT′ and $MLCT^2$ is equivalent to MLCT″, the latter conventions being those used in Olsen et al. [15].

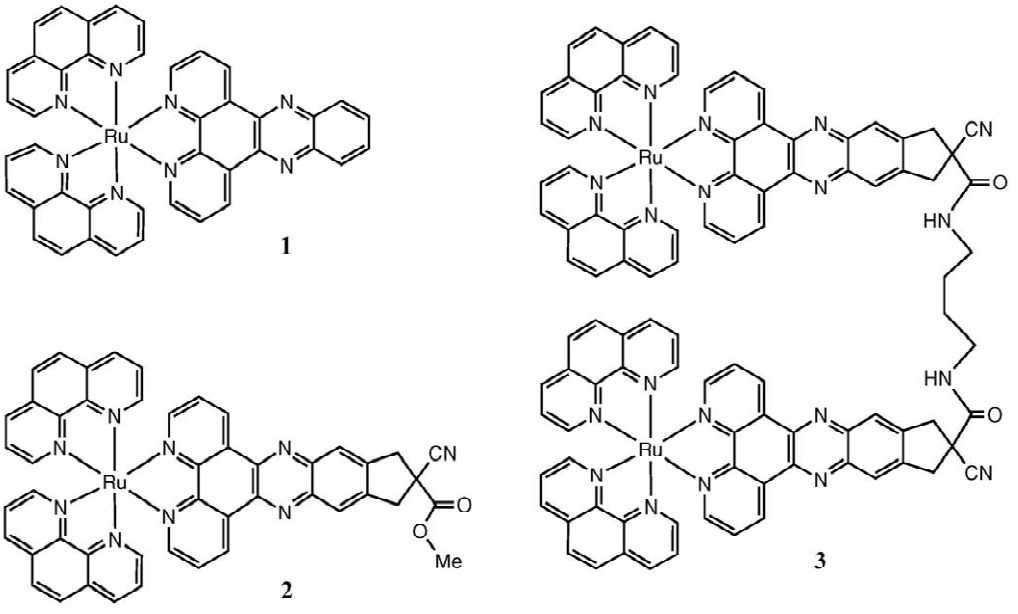

Fig. 1. Structures of the ruthenium complexes. $[Ru(phen)_2dppz]Cl_2$ (**1**), $[Ru(phen)_2cpdppzOMe]Cl_2$ (**2**) and $[\mu\text{-}C4(cpdppz)_2\text{-}(phen)_4Ru_2]Cl_4$ (**3**). Note that the metal centre is chiral which results in three diastereoisomers (Δ-Δ, Λ-Λ, and Λ-Δ=*meso*) for **1**, and two enantiomers (Δ and Λ) for **2** and **3**.

2.2. Picosecond TR³, including Kerr cell measurements

The ps-TR³ set-up at RAL has been described in detail elsewhere [28]. The apparatus uses a regenerative amplifier system providing a 1 ps, 800 nm fundamental pulse (2–3 mJ), which is frequency doubled to pump an optical parametric amplifier (OPA) generating a probe pulse at 1 kHz.

Four combinations of pump and probe pulses with pulse duration of 1 ps were employed: 400 nm pump/322 nm probe (10 μJ and 3–4 μJ, respectively), 400 nm pump/350 nm probe (pulse energies 10 and 3–4 μJ, respectively), 390 nm pump/520 nm probe (~5 and ~5 μJ, respectively), and 390 nm pump/390 nm probe (10 and 6 μJ, respectively). The 390 nm pulses were obtained by frequency doubling the fundamental tuned to 780 nm. Each pulse had a spot diameter of ~300 μm at the sample. The 400 nm/350 nm and 400 nm/322 nm combinations were used without Kerr gate but with a Triplemate three-stage spectrometer in place. The 390 nm/520 nm and 390 nm/390 nm combinations were used with the Kerr gate in order to eliminate, respectively, luminescence and Raman signal from the pump pulse. A single-stage spectrometer in combination with a 410 nm liquid filter (diphenylanthracene in cyclohexane) was employed with this particular arrangement. The ps-TR³ signal was collected at 90° geometry, dispersed through a spectrograph and detected by a liquid nitrogen cooled CCD. The pump and probe had parallel polarizations relative to each other. The spectral resolution is ~30 cm^{-1}.

The Kerr gate [25] was developed fundamentally for efficient rejection of fluorescence from Raman signals, the fast gating arising from induced transient anisotropy of a CS_2 Kerr medium, in a 2 mm cell, driven by a residual fundamental laser pulse (1 ps, 500 μJ), focused to a 1–2 mm diameter spot with gating time ~4 ps (full width at half maximum, FWHM). The requirement of the gate in the current investigation, however, was not so much to reduce background fluorescence, but to enable the use of a single wavelength (390 nm) pump/probe arrangement by eliminating the Raman signal arising from the pump beam. With the Kerr cell in place, the minimum pump-probe delay was effectively limited to 4 ps, below which there was significant leakage of pump Raman signal through the gate. For pump-probe delay times of 4 ps, it was necessary to subtract a spectrum recorded with pump only at the corresponding time delay, in order to correct for 'leakage' through the Kerr gate of Raman signal arising from the pump. The spectra presented in this paper are pure excited state spectra which have been corrected for ground-state scattering through scaled subtraction of the sample spectrum obtained at negative pump/probe time delay (−20 ps), and for solvent scattering by subtraction of the solvent only spectrum obtained also at −20 ps pump/probe time delay. In water, ground state spectra were subtracted before solvent spectra. In organic solvents, solvent spectra were subtracted before ground state spectra. Examples of the data before ground state subtraction can be seen in Ref. [24]. The data are generally presented as raw data. However, it is possible to fit the spectra with a series of Gaussian curves to simulate the Raman bands. This was done for several sets of high quality data that were collected with extensive averaging, as presented in Fig. 10.

The sample was presented as a vertically flowing open jet (500 μm diameter) which required sample volumes of ~50 ml. In non-aqueous solvents, the samples exhibited

decolouration after extended experimentation (1–2 h), and were regularly replaced. However, samples in water and bound to DNA were stable and could be used for several days. The data presented were collected with extensive averaging to obtain reasonable S/N. For a single spectrum, typically 3–10 data sets were averaged over a total collection period of 10–80 min, depending on signal intensity. If the data appeared to deteriorate with run-time, the sample was renewed and poor data were not included in the averages. In kinetic experiments, the time delays were randomly varied.

3. Results

3.1. TR^3 spectra of $[Ru(phen)_2dppz]Cl_2$ in aqueous solution: variation of probe wavelength

TR^3 spectra were recorded for aqueous solutions of $[Ru(phen)_2dppz]Cl_2$ probing at 322, 350 and 390 nm (Fig. 2).

The spectral intensities at all three wavelengths were high, with the best S/N at 350 nm, and good quality spectra were obtained with 20 ps delays. According to previous reports [15,16], the lowest excited state of the complex in water is formed with a lifetime of 3–4 ps. Therefore, a spectrum recorded at 20 ps delay is expected to reflect only that state (as confirmed by our kinetic studies).

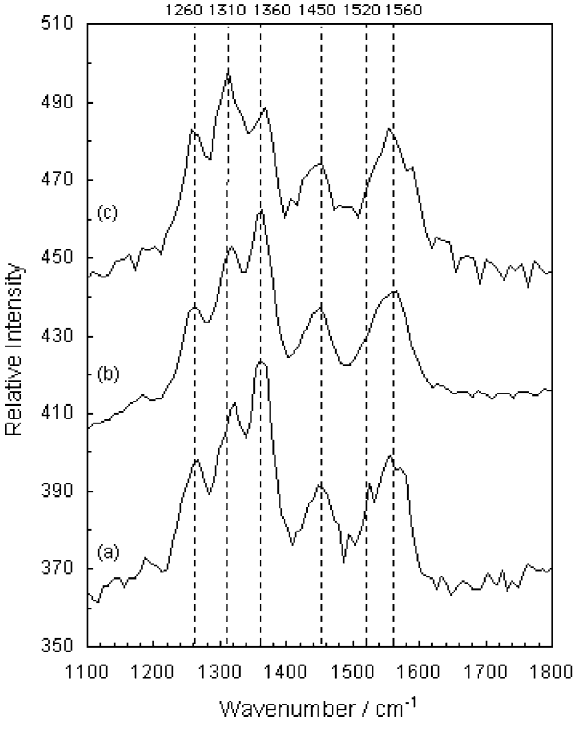

Fig. 2. Comparison of TR^3 spectra for $[Ru(phen)_2dppz]Cl_2$ in H_2O at a delay of 20 ps with different probe wavelengths. Experimental conditions were: (a) pump 390 nm/probe 390 nm, (b) pump 400 nm/probe 350 nm, (c) pump 400 nm/probe 322 nm.

The spectra at the three probe wavelengths are similar but exhibit different enhancement patterns. In particular, the bands at 1260 and 1310 cm^{-1} become more pronounced as the probe wavelength becomes shorter.

For comparison with previous work [24], a TR^3 spectrum was recorded of $[Ru(bpy)_2dppz](BF_4)_2$ probing at 390 nm with a 20 ps delay (supplementary material[2]). The spectrum was similar to that of $[Ru(phen)_2dppz]Cl_2$, consistent with the lowest excited state being localised on the dppz ligand. Whilst non-polypyridyl ancillary ligands can strongly influence the photophysics of ruthenium(II)-dppz complexes [29–31], it was expected that complexes with phen and bpy as ancillary ligands would have very similar properties. These complexes have been compared previously using ns-TR^2 spectroscopy which allowed the phen, bpy and dppz modes to be distinguished [20].

3.2. TR^3 spectra of $[Ru(phen)_2dppz]Cl_2$ in aqueous solution: kinetics

The temporal evolution of the TR^3 spectrum of $[Ru(phen)_2dppz]Cl_2$ in water was examined with probe wavelengths of 350 and 390 nm.

The signals were strongest at 350 nm and the grow-in of the final spectrum is clear, with little or no change in the spectral profile from 1 to 20 ps (Fig. 3). However, closer examination reveals a shift in the band at 1520–1560 cm^{-1} between 5 and 20 ps delays. This may indicate that a state with more intensity at lower wavenumbers is formed initially and then disappears. A band at 1526 cm^{-1} has earlier been identified as a marker band for the luminescent state that dominates in organic solvents and DNA [20].

Two methods of analysis were used to extract kinetic parameters from the data. Firstly, the integrated intensity of several excited state peaks was plotted versus time and there appeared to be a ~1 ps delay before the signal started to evolve (Fig. 4). To take account of cross-correlation, the pulse width was obtained by fitting the evolution of ground-state bleach (FWHM 3 ps for combined pump and probe cross correlation time). Subsequent fitting of the data with pulse deconvolution revealed a risetime of 6 ps with the start of the grow-in fitted to +0.8 ps. In a complementary approach, using principal component analysis, the major contribution to the spectrum was fitted to have a rise of 3 ps. A lifetime of 3–6 ps is consistent with those reported for the formation of the lowest excited state of $[Ru(phen)_2dppz]Cl_2$ in water using transient absorption [15,16]. It is likely that the fitted delay of 0.8 ps correlates

[2]Supplementary material is available at http://www.ncl.ac.uk/chemistry/research/publications/emt_publications.html and also (supplementary figures) at the Elsevier website http://www.elsevier.com/homepage/saa/jib.

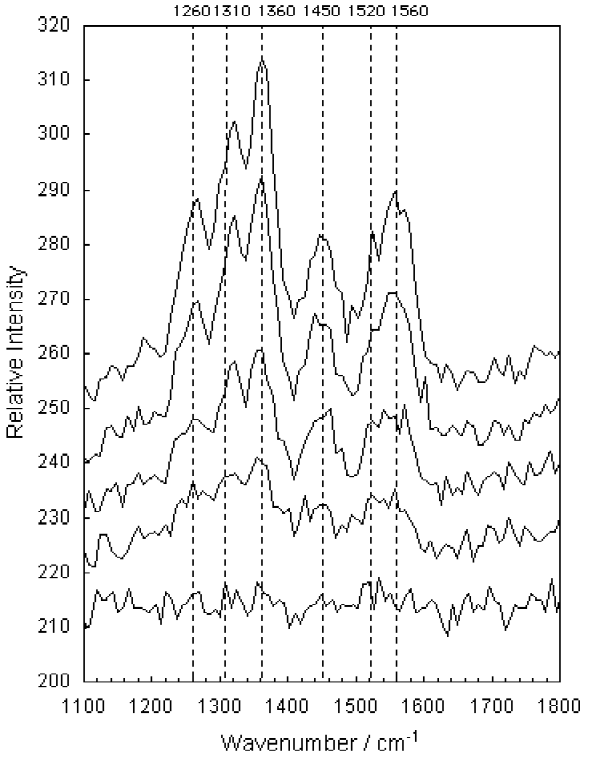

Fig. 3. Temporal evolution of TR^3 spectrum for $[Ru(phen)_2dppz]Cl_2$ in H_2O at delays of, from bottom, 0, 3, 5, 11 and 20 ps. Pump 400 nm/probe 350 nm.

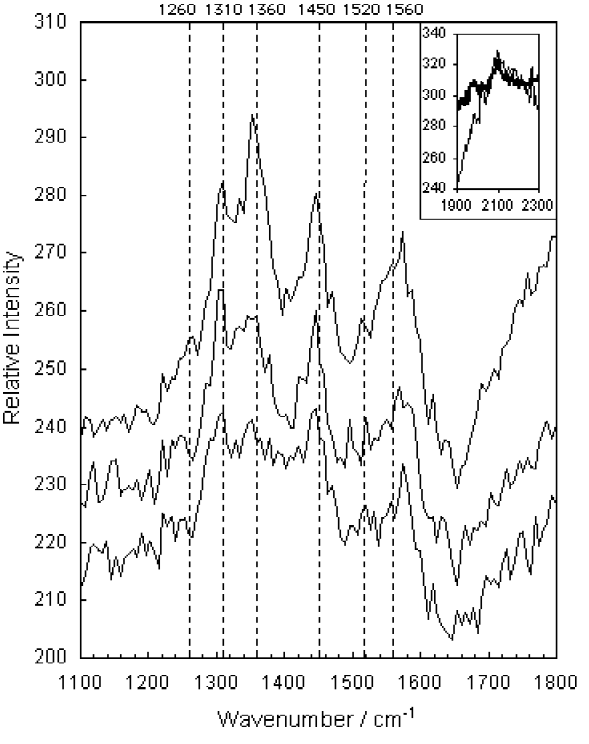

Fig. 5. Temporal evolution of TR^3 spectrum for $[Ru(phen)_2dppz]Cl_2$ in H_2O. The time delays are, from bottom, 4, 6 and 20 ps. Pump 390 nm/probe 390 nm. The inset shows the TR^3 spectra at 20 ps of $[Ru(phen)_2dppz]^{2+}$ (thick line) and $[Ru(bpy)_2dppz]^{2+}$ (thin line) in the high wavenumber region. The band at 2100 cm^{-1} is observed only in aqueous media for delays >10 ps.

with the 0.7 ps species observed by Önfelt et al. [16] with the initial species having no resonance at this probe wavelength.

A grow-in of the signal also occurs with the 390 nm probe (Fig. 5) although, because of the Kerr gate, 4 ps is the lower limit for the time delay in this case. Under these conditions, the spectral profile clearly changes as the signal grows with time. A cursory inspection reveals that the relative intensities of a number of peaks change between 4 and 20 ps delays, i.e. the peak intensities of the bands at 1310 and 1360 cm^{-1} are inverted, and the band at 1560 cm^{-1} gains in intensity relative to that at 1520 cm^{-1}. Similar changes are observed in D_2O (supplementary material (see footnote 2)).

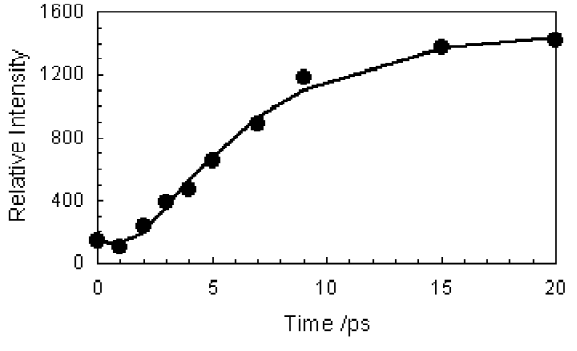

Fig. 4. Kinetics of the rise of the TR^3 signal for $[Ru(phen)_2dppz]Cl_2$ in H_2O with 400 nm pump and 350 nm probe, where the integrated peak intensity (1366 cm^{-1}, ●) is plotted against delay time. The error for each data point is ±10%. The solid line represents a monoexponential fit to the data with pulse (FWHM 3 ps) deconvolution, yielding a lifetime of 6 ps for the rise preceded by a delay of 0.8 ps.

One other feature of note that was present only in spectra of the lowest excited state (i.e. the spectra at delays beyond 15 ps) of either $[Ru(phen)_2dppz]Cl_2$ or $[Ru(bpy)_2dppz](BF_4)_2$ in H_2O (or D_2O) and only with 390 nm probe, was a band at ~2100 cm^{-1} (inset, Fig. 5). There is no band in this position in the ground-state spectra of these complexes, nor is there any feature at this position in the ground or excited state spectra of $[Ru(bpy)_3]Cl_2$ recorded under identical conditions. It may be a combination band but otherwise its origin is unclear. However, it is identifiable with this particular state and no other, but we will not discuss this spectral feature further.

3.3. TR^3 spectra of $[Ru(phen)_2dppz]Cl_2$ in non-aqueous solution: acetonitrile and ethanol

TR^3 spectra were recorded for solutions of $[Ru(phen)_2dppz]Cl_2$ in acetonitrile probing at 350 and 390 nm. Attempts to probe at 522 nm failed due to low signal intensity. Raman spectra were much stronger when probing at 390 compared to 350 nm. It was not clear why the

signals with 350 nm probe are of such low intensity since, assuming the excited state absorption does not change after 1 ps as previously reported [15], the excited state absorption at 350 nm is about double that at 390 nm (Fig. 6) while that at 522 nm is very low.

The raw data contained strong background contributions from both the ground state complex and solvent making it impossible to extract the excited state spectrum at 350 nm. Probing at 390 nm, comparison of spectra at 4, 20 and 100 ps delays showed no discernable indication of a grow-in or change of spectral profile with time (supplementary material (see footnote 2)). However, it was impossible to state this conclusively because of uncertainties inherent in judging the solvent and ground state contributions that should be subtracted from the TR^3 spectra. Thus, our emphasis was on obtaining a high quality spectrum at 20 ps delay with 390 nm probe to compare with the equivalent spectrum in water. Later work using CD_3CN as solvent has shown an evolution of the spectrum in acetonitrile with a lifetime of ~20 ps [32] which was also observed in transient absorption [33]. It is not clear why this evolution was not observed in previous transient absorption work [15], but it may be that the conversion was not apparent at the chosen probe wavelengths.

To investigate further the evolution of the non-emissive state in water, we examined a mixture of acetonitrile and water as solvent, as reported in transient absorption studies [15]. TR^3 spectra were recorded for solutions of $[Ru(phen)_2dppz]Cl_2$ in acetonitrile/water (1:2, v/v) probing at 390 nm, with delays of 4, 6, 10, 20, and 50 ps (supplementary material[3]). As anticipated, the evolution was similar to that observed in pure water but on a slower timescale.

For comparison with previously published work [24], a TR^3 spectrum was recorded for a solution of $[Ru(bpy)_2dppz](BF_4)_2$ in acetonitrile probing at 390 nm. At 20 ps delay, the spectrum was not significantly different from that of $[Ru(phen)_2dppz]Cl_2$, consistent with the excited state being localised on the dppz ligand.

TR^3 spectra were recorded for solutions of $[Ru(phen)_2dppz]Cl_2$ in ethanol probing at both 350 and 390 nm. As with acetonitrile, the signal intensity with 390 nm probe was much greater than with 350 nm probe. Also in common with acetonitrile, the strong background signals from the solvent as well as the ground state made it difficult to obtain the pure excited state spectra. Nonetheless, it was clear that the signal evolved with time even though it was impossible to judge whether there was a concomitant change in the spectral profile. With a 350 nm probe, it was possible to obtain kinetic data by analysing the change in intensity with time in several regions of pure strong excited state absorption (Fig. 7). Although these data were not amenable to kinetic analysis, the grow-in is on a timescale similar to that observed in acetonitrile and methanol [32].

3.4. TR^3 spectra of $[Ru(phen)_2cpdppzOMe]Cl_2$ and $[\mu$-$C4(cpdppz)_2(phen)_4Ru_2]Cl_2$: variation of probe wavelength and solvent

TR^3 spectra were also recorded for the complexes that we have modified to improve their DNA binding properties

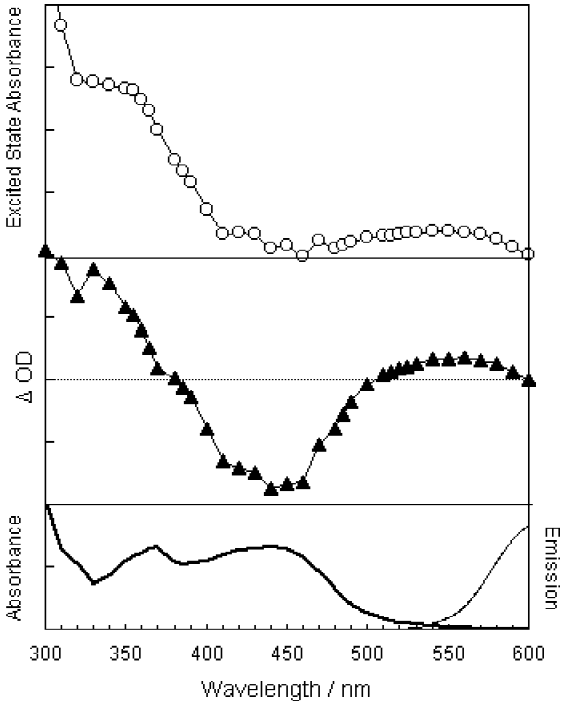

Fig. 6. Nanosecond transient absorption (–▲–) spectrum of Λ-$[Ru(phen)_2(dppz)]Cl_2$ in argon-purged CH_3CN (τ_{decay} = 650 ns). The error for each data point is ±20%. For comparative purposes the ground state absorption (thick line) and emission spectra (thin line) are shown below. Also shown above is an estimated excited state spectrum (–○–) obtained as a linear combination of the absorption and transient absorption spectra, calculated to eliminate depletion at 450 nm. Lines are not fits but are drawn to guide the eye.

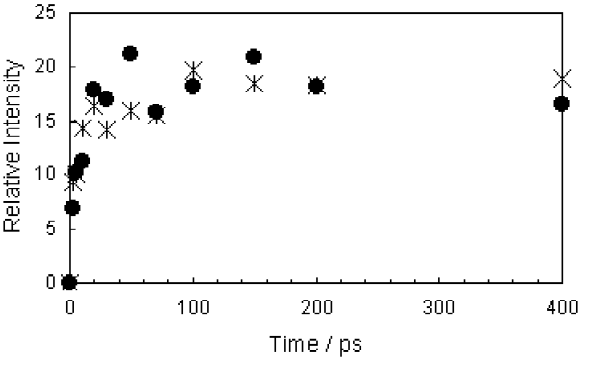

Fig. 7. Kinetics of the rise of the TR^3 signal for $[Ru(phen)_2dppz]Cl_2$ in EtOH with 400 nm pump and 350 nm probe, where maximum peak intensities at 1355 cm^{-1} (*) and 1589 cm^{-1} (●) are plotted against delay time. The error for each data point is ±25%. The initial fast rise is due to the pulse (FWHM 3 ps) and the rise thereafter represents the grow-in of the excited state resonance Raman signal.

[26,27], since much of our complementary transient absorption studies have focused on a similar monomer and the same dimer [16]. It was also interesting to investigate the effect of alkylation at the 11,12-positions since modification at these positions may affect the photophysics of the complex [34]. However, it appears that alkylation has minimal electronic influence since the TR^3 spectra of these complexes in H_2O and CH_3CN with both 350 and 390 nm probes were essentially identical to those of $[Ru(phen)_2dppz]Cl_2$. The temporal evolution patterns for the spectra probing at 350 and 390 nm were likewise similar to the standard monomer, as shown in Fig. 8 for $[Ru(phen)_2cpdppzOMe]Cl_2$ where the shift with time of the 1560 cm^{-1} band with a 350 nm probe can be observed.

3.5. TR^3 spectra of $[Ru(phen)_2dppz]Cl_2$ bound to DNA: variation of P/D ratio

TR^3 spectra were recorded at time delays of 4, 20, and 100 ps for solutions of rac-$[Ru(phen)_2dppz]Cl_2$ bound to calf-thymus DNA (CT-DNA) with both pump and probe at 390 nm (Fig. 9A,B). The racemate was used to allow comparison with previously published transient absorption data [15]. Since the photophysics on the nanosecond timescale for $[Ru(phen)_2dppz]Cl_2$ bound to DNA are sensitive to factors such as *P*/*D* ratio [10,12], various

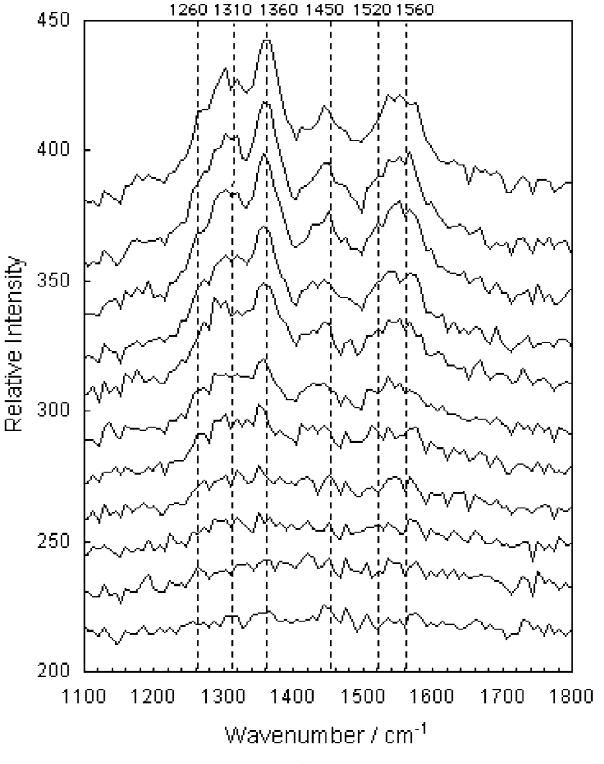

Fig. 8. Temporal evolution of TR^3 spectrum for $[Ru(phen)_2cpdppz-OMe]Cl_2$ in H_2O. The time delays are, from bottom, 0, 1, 2, 3, 4, 5, 7, 9, 12, 15 and 20 ps. Pump 400 nm/probe 350 nm.

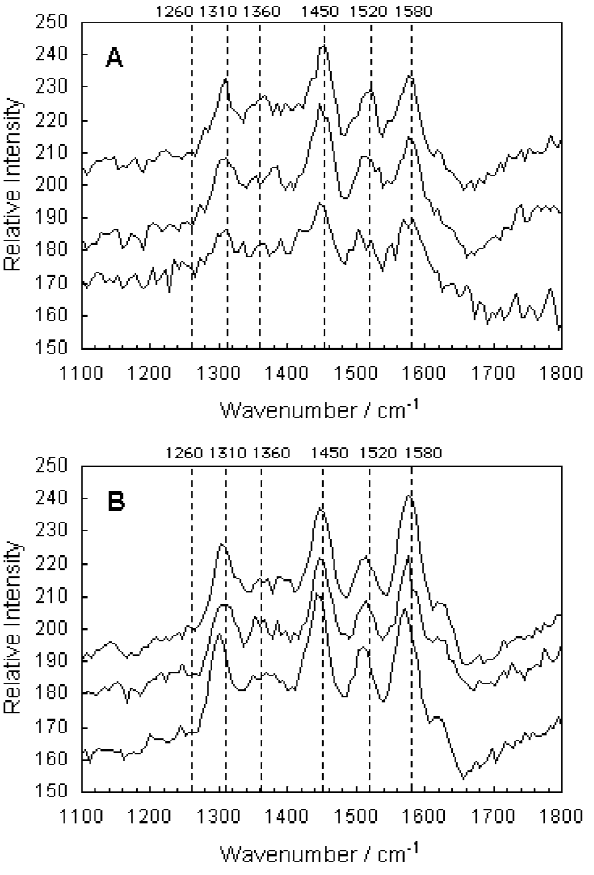

Fig. 9. (A) Temporal evolution of TR^3 spectra for $[Ru(phen)_2dppz]Cl_2$ bound to CT-DNA (5 mM phosphate buffer) at $P/D = 8.5$ ($[Ru^{2+}] = 0.6$ mM). Spectra were recorded at time delays of, from bottom, 4, 20 and 100 ps. Pump 390 nm/probe 390 nm. (B) Comparison of TR^3 spectra at 20 ps delay for $[Ru(phen)_2dppz]Cl_2$ bound to sonicated CT-DNA (5 mM phosphate buffer) at three *P*/*D* ratios, from bottom, $P/D = 5.4$, $[Ru^{2+}] = 0.9$ mM; $P/D = 8.5$, $[Ru^{2+}] = 0.6$ mM; $P/D = 9.7$, $[Ru^{2+}] = 1$ mM, delay = 20 and 4 ps. Pump 390 nm/probe 390 nm.

sample conditions were examined: P/Ru = 8.5 ([Ru] = 0.6 mM), P/Ru = 5.4 ([Ru] = 0.9 mM), and P/Ru = 9.7 ([Ru] = 1.0 mM). No difference could be distinguished between the spectra for the three samples.

There was a rise of the signal with time from 4 to 20 ps, but the spectra at 20 and 100 ps were of equal intensity (Fig. 9B). This is consistent with our previous TA observations for Δ-$[Ru(phen)_2dppz]Cl_2$ bound to CT-DNA [16] although no kinetics on this timescale were reported in TA studies of rac-$[Ru(phen)_2dppz]Cl_2$ bound to DNA [15]. However, there is no change in spectral profile as the signal evolves on this timescale. The shapes of the spectra at all the time delays investigated are essentially identical, and show features identified with the luminescent state of the chromophore [20], such as an intense band at ~1520 cm^{-1}. We observe no evolution of the spectrum with DNA beyond 100 ps and indeed the TR^3 spectrum at 100 ps closely resembles the reported ns-TR^2 spectrum [20].

4. Discussion

4.1. Three excited states identified in water

On the basis of transient absorption studies, Barbara and coworkers [15] suggested that $[Ru(phen)_2dppz]Cl_2$ has two close-lying excited states termed $MLCT^1$ and $MLCT^2$. $MLCT^1$ is analogous to the ^3MLCT states commonly observed for ruthenium tris(polypyridyl) complexes which luminesce moderately around 615 nm. $MLCT^2$ is a second state that lies higher in energy than $MLCT^1$ in most solvents but is lower in water where very weak luminescence around 800 nm is observed. It was proposed that $MLCT^1$ is populated prior to $MLCT^2$ in aqueous solution but the conversion is rapid (3 ps). Önfelt et al. [16] found that in addition to the 3 ps process (and its subsequent decay in 250 ps), a third process could be identified in water. This was very rapid (0.7 ps) with a large associated change in anisotropy, and it was suggested that it may be due to a funneling to the dppz ligand of those excited states that were formed by an initial charge transfer to the phenanthroline ligands. We anticipated that TR^3 could be used to identify the spectral characteristics of $MLCT^1$ and $MLCT^2$ by measuring the temporal evolution of the spectra in water but considered that the 0.7 ps transient (a 'precursor' state) was too short-lived to be identifiable given the temporal limitations of the technique. However, we believe that from the combination of probe wavelengths used we can in fact observe all three species in our data.

If the hypothesis of two excited states, with $MLCT^1$ occupied initially in all solvents, is correct, then in aqueous solution a different spectrum should be observed at 1–4 ps than at 20 ps, and the initial spectrum should have features more in common with that observed in DNA and acetonitrile. However, this is complicated by the fact that, despite the complex luminescing strongly at ~615 nm in both DNA and acetonitrile, the spectra in these solvents are far from identical [32]. Nonetheless, two resonance Raman features have been identified in the literature as being characteristically distinct for the luminescent state. One is the observation of a band at 1526 cm^{-1} [20] which has been described as a qualitative marker for the state that luminesces strongly at ~615 nm ($MLCT^1$): it is observed in DNA and acetonitrile while it is absent in water at longer times. The other characteristic is the position of the band observed at 1390 cm^{-1} in acetonitrile which is shifted to 1361 cm^{-1} in water [24]: the position of this band in the DNA spectrum is unclear however, since it is too weak to be clearly distinguishable from the background. With respect to both these features, when probing at 390 nm, we observe that the spectrum in water at 4 ps resembles more closely the spectrum in DNA than the 20 ps spectrum in either water or acetonitrile (Fig. 10).

Probing at 350 nm, however, there is little distinguishable difference between the spectral shapes in water at long and short time delays, although at short times there is a higher relative intensity at 1520 cm^{-1} as also observed probing at 390 nm. On the other hand, the TR^3 spectrum of $[Ru(phen)_2dppz]Cl_2$ grows-in strongly at this probe wavelength from no detectable signal at 1 ps and when the kinetics are analysed to take account of the pulse, a 0.8 ps delay in the grow-in (6 ps) is observed. By analogy with the 0.7 ps process observed in transient absorption [16], it is likely that this delay is due to the conversion from the 'precursor' state to $MLCT^1$, with both these states being poorly resonant at 350 nm. Poor resonance of $MLCT^1$ compared to $MLCT^2$ at 350 nm by contrast with 390 nm concurs with the observed weak spectra obtained in acetonitrile when probing at 350 nm compared to 390 nm. Furthermore, a grow-in of the spectrum in acetonitrile on the ps timescale from a poorly resonant state at both 350 and 390 nm has been recently reported [32]. Hence, the slowest kinetics in water reflect predominantly the kinetics for population of $MLCT^2$.

We observe no detectable difference between the spectra of $[Ru(phen)_2dppz]Cl_2$ in H_2O or D_2O, and the rise of the signal between 4 and 20 ps appears identical. Therefore, if stabilization of $MLCT^2$ does involve H-bonding at the phenazine nitrogens, this interaction has no discernable influence on the resonance Raman spectrum. A solvent isotope effect (τ_{D_2O}/τ_{H_2O}) of 1.25 has been measured by transient absorption for this process [16], which could be correlated with the isotope effect reported for the reorientation of water at room temperature [35]. However, this difference could not be distinguished from the TR^3 data. This may be compared with the larger isotope effect of ~2.3 on the decay of the lowest excited state of

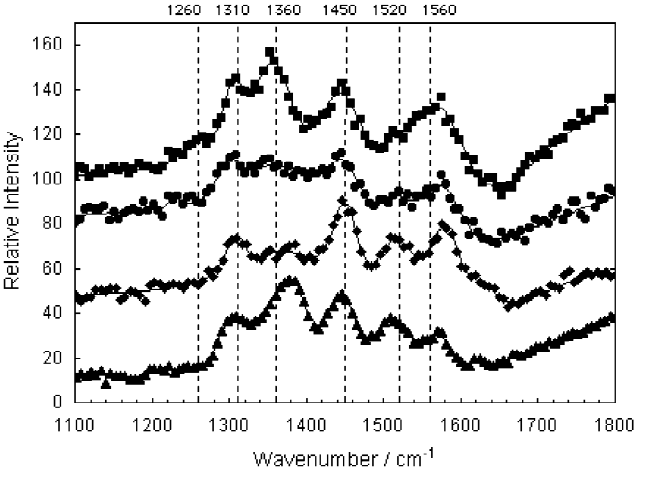

Fig. 10. Comparison of TR^3 spectra for $[Ru(phen)_2dppz]Cl_2$ in various environments with pump 390 nm/probe 390 nm. From bottom: in CH_3CN at 20 ps delay (▲), bound to CT-DNA ($P/D = 8.5$) at 20 ps delay (♦), in H_2O at 4 ps delay (●), and in H_2O at 20 ps delay (■). Symbols represent the experimental data and solid lines represent fits to the data using Gaussian curves to simulate the Raman bands.

$[Ru(phen)_2dppz]Cl_2$ in H_2O and D_2O [15], which although consistent with the notion that differential hydrogen-bonding to the ground and excited states may be involved in the decay, was not definitive since an isotope effect of similar magnitude had been observed for $[Ru(bpy)_3]^{2+}$ [36].

4.2. Two states in non-aqueous media

To investigate further the evolution of the non-emissive state in water, we examined a (1:2, v/v) mixture of acetonitrile and water as solvent. According to Barbara and coworkers [15], the transient absorption in this medium resembles that in pure water but increasing amounts of acetonitrile lead to slower overall kinetics for population of $MLCT^2$. Thus, for acetonitrile/water (1:2, v/v) as solvent, emission from the different states had lifetimes of 10 ps ($MLCT^1$) and 950 ps ($MLCT^2$) [15]. Although a kinetic analysis of our limited data set was not feasible, it is clear that the kinetics are slower in the mixed solvent than in pure water, with the evolution of the final spectrum not complete until 50 ps in the CH_3CN/H_2O mixed solvent compared to 20 ps in H_2O. However, other than the slower kinetics, the evolution of the spectrum is very similar to that observed in pure water.

However, the interpretation of data in this mixed solvent medium is complicated by the recent finding that the TR^3 spectrum of $[Ru(phen)_2dppz]Cl_2$ in CD_3CN itself develops on the timescale of tens of picoseconds [32]. This was an unexpected finding since generally solvation processes in acetonitrile are extremely rapid [37]. Spectral evolution on a similar timescale was also observed in methanol [32]. These kinetics were assigned to the conversion of 'precursor' to $MLCT^1$. We report here that in ethanol the TR^3 spectrum similarly grows in with a lifetime on the order of tens of picoseconds.

It is possible that these grow-ins correspond to the 0.7 ps conversion observed in water [16] which we have assigned as a 'precursor' to $MLCT^1$ conversion, although no subsequent conversion to a state resembling $MLCT^2$ was observed in non-aqueous solution. We cannot exclude, however, that they reflect a different process, perhaps solvation of $MLCT^1$.

4.3. Excited state dynamics with DNA

For $[Ru(phen)_2dppz]Cl_2$ bound to CT-DNA there was an increase in resonance with time between 4 and 20 ps, but the spectra at 20 and 100 ps were essentially identical in intensity. The slow molecular rotation process [16] cannot be expected to play a part in spectral changes that occur on sub-20 ps timescales. Therefore, the increase in signal intensity at early times could reflect either an increase in population of a state or an enhancement in the resonance Raman excitation cross-section brought about through changes in energy following relaxation processes (e.g. IVR, solvation, etc.). In transient absorption and anisotropy measurements [16], a biexponential evolution of the long-lived (hundreds of nanoseconds) signal was observed with lifetimes of 7 and 37 ps. Insufficient TR^3 data were collected for lifetime analysis but the observed grow-in undoubtedly reflects the same processes that are observed in transient absorption. Because of the small changes in ΔOD and anisotropy observed at all times, it was proposed that the kinetics were due to a rearrangement of the bound $[Ru(phen)_2dppz]Cl_2$ complex in its intercalation pocket after excitation rather than an interconversion between states [16]. The two lifetimes were suggested to be related to the reorganisation time of DNA, which is anticipated to be slower than that of other solvents because of steric and conformational constraints. The fact that the TR^3 spectrum remained unchanged during its evolution indicates that it is the same excited state that is observed during the evolution, and supports this proposal. Hence, the changes in anisotropy and transient absorption observed by Önfelt et al. [16] and the rise in signal intensity observed in our TR^3 spectra both likely reflect reorganisation of the metal complex in its intercalation pocket in order to minimize the energy of the bound excited state; this may lead to a small increase in the absorption of the excited state and hence stronger resonance for TR^3 spectra.

We suggest now that in addition to solvent reorganisation being important for relaxation of the excited state, counterion reorganisation may also be required. Because the DNA counterions are essentially spatially fixed, this may explain why the TR^3 spectrum of $[Ru(phen)_2dppz]Cl_2$ bound to DNA remains identical at all delays with a slow progression to the final resonance. Rather than mobile counterions reorganising around the excited state, the complex must undergo nuclear rearrangements to accommodate the redistribution of electronic charge brought about by formation of the MLCT state. In particular, it adjusts to minimize unfavourable interactions with the phosphate groups and the effect of placing a negative charge between the stacked bases while maintaining its favourable intercalative binding arrangement.

One reason for this postulate is consideration of a process with slow kinetics in acetonitrile that has been postulated to reflect formation of the $MLCT^1$ excited state [32]. Generally any process limited by non-diffusive solvent reorganisation occurs on a sub-picosecond timescale in acetonitrile, but for this system it appears to occur on the timescale of tens of picoseconds and is slower than in water for which the reorganisation is hindered by H-bonding. One possible explanation for this would be if counterion relaxation were limiting since ion-pairing would be more influential in the lower dielectric medium. Indeed, in glasses, a fluorescence anisotropy higher than predicted for D_3-symmetry is observed for $[Ru(bpy)_3]^{2+}$ which has been attributed to the effect of ion-pairing [38,39].

4.4. Comparison of TR^3 spectra of $[Ru(phen)_2dppz]Cl_2$ in water, acetonitrile, and CT-DNA

Fig. 10 shows a comparison of the excited state spectra of $[Ru(phen)_2dppz]Cl_2$ in different environments probed at 390 nm. Despite the complex being strongly luminescent at ~615 nm in both acetonitrile and DNA, the TR^3 spectra after equilibration to the lowest excited state are not the same in the two solvents. However, they do share some features that distinguish them from the spectrum of the lowest excited state in water, as discussed previously with respect to the 4 ps spectrum in water. The spectrum in environments that stabilise the luminescent state is characterised by the band at ~1366 cm^{-1} being shifted to longer wavenumber compared to the spectrum in water at long delays, and by the presence of the band at 1526 cm^{-1} that is distinctive for non-aqueous environments [20].

However, what is most remarkable is that the spectrum of $[Ru(phen)_2dppz]Cl_2$ observed in water at 4 ps, closely resembles that of the complex bound to DNA. This suggests that the DNA spectrum represents an essentially unsolvated MLCT state localised on dppz.

Our model of the states involved in the photophysics of Ru in various media is shown in Scheme 1.

4.5. Nature of the 'precursor' state

When the TR^3 data presented here are considered in the context of recent transient absorption and resonance Raman studies of $[Ru(phen)_2dppz]Cl_2$ [15,16,24,32,33] and similar studies of $[Ru(bpy)_3]^{2+}$ [40–45], a model can be constructed for the processes that occur in the excited state of $[Ru(phen)_2dppz]Cl_2$ depending on its environment.

Considering the relative intensities of ps-TR^3 and ns-TR^2 spectra in acetonitrile, it is clear that the state designated $MLCT^1$ is poorly in resonance at 350 nm compared to 390 nm. The state designated $MLCT^2$, observed in water at long delays, has good resonance at both 350 and 390 nm. Since the spectra in water at short delays are more intense at 390 than 350 nm and moreover show a feature at 1520 cm^{-1} which is associated with a luminescent state of the complex, it is likely that $MLCT^1$ is populated prior to $MLCT^2$ in water. The lifetimes extracted from TR^3 spectra (3–6 ps) correlate with those calculated from transient absorption (3–4 ps) for this process. Thus, it appears that $MLCT^1$ is populated in all solvents, consistent with the model proposed by Barbara et al. [15], and that in water there is a subsequent conversion to $MLCT^2$. However, it does appear that $MLCT^1$ is differently solvated in different media since at long delays distinctly different TR^3 spectra are observed in the non-aqueous environments of MeOH, CH_3CN, and DNA [32].

However, the Barbara model does not account for all the experimental observations since the accumulated evidence appears to point to the existence of another state, which we have termed the 'precursor' state, that precedes or is coexistent with $MLCT^1$ in all solvents. Since the formation of $MLCT^1$ is always observed as a grow-in, this state is apparently in poor resonance at all probe wavelengths used. We can correlate our TR^3 findings with those from transient absorption in water where an initial state is observed that converts to another state in 0.7 ps: it is likely that the initial state is equivalent to our 'precursor' and the subsequent state to $MLCT^1$. Notably, a process with this lifetime is observed in our TR^3 data for the delay in formation of $MLCT^1$ in water probing at 350 nm. TR^3 data have also revealed the occurrence of a grow-in of $MLCT^1$ in acetonitrile and methanol [32], which has been postulated to represent the same 'precursor' to $MLCT^1$ conversion. The question then is what is the nature of the 'precursor' state and what process could be occurring on this timescale.

It may be noted that time constants of 1–100 ps are of the same order of magnitude as those reported for inter-ligand electron transfer (ILET) in $[Ru(bpy)_3]^{2+}$ measured using time-resolved resonance Raman and polarization techniques [40–45][3]. Indeed, it was suggested that the 0.7 ps process for $[Ru(phen)_2dppz]Cl_2$ in water could be due to charge transfer from the phen ligands to the dppz ligand if the MLCT can be initially localised on any ligand [16]. It seems clear that the lowest excited state in any solvent, $MLCT^1$ or $MLCT^2$, is localised on the dppz ligand. However, there is no reason to believe that the Franck–Condon state is likewise localised on dppz. In fact, a resolution of the absorption envelope of $[Ru(phen)_2dppz]Cl_2$ reveals four effective polarization directions along one of which any transition is polarized

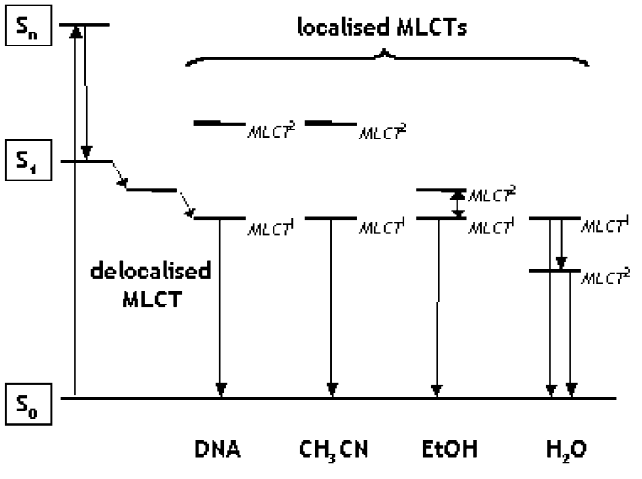

Scheme 1.

[3]The evolution of the TR^3 spectrum of $[Ru(bpy)_3]Cl_2$ in water was measured as a control with 350 nm probe since it was expected that formation of the ^3MLCT would be complete by 1 ps [41]. However, the excited state signal appeared to evolve over 20 ps, perhaps reflecting ILET which is reported to have a lifetime of ~15 ps [38].

[46]. Either in solution or bound to DNA, at the excitation wavelengths used for TR^3 studies (390 and 400 nm), only ~40% of the absorption is polarized purely parallel to the dppz long axis; in previous transient absorption experiments [16] ($\lambda_{ex}=502$ nm) ~70–80% of the absorption was polarized in this direction. Thus, excitation will involve all three ligands. By analogy with $[Ru(bpy)_3]^{2+}$, it is likely that the Franck–Condon state for $[Ru(phen)_2dppz]Cl_2$ will consist of ^{1}MLCT states localised on any one of the three ligands which will convert rapidly (τ~100 fs) to the corresponding localised ^{3}MLCT states [43–45]. Such processes are fast and are likely to be associated with the inertial solvent response which is very rapid for acetonitrile and sub-picosecond for many solvents [37]. Indeed, a time constant of τ~60 fs is observed for such processes in $[Ru(bpy)_3]^{2+}$ in CH_3CN [43][4].

However, it is after this equilibration that ILET would lead to the final localisation of the ^{3}MLCT on dppz. Considering the large dipole moment established by creating the MLCT, the change of dipole due to ILET would be strongly coupled to the polarization of the local solvent and depend on the diffusional reorganisation of solvent. We cannot exclude the possibility that counterion reorganisation is also coupled to ILET and solvent reorganisation, and we consider that this could possibly be rate-limiting. We have already discussed the restrictions on reorganisation of the bases and the phosphate 'counterions' in this system (Section 4.3) which results in $MLCT^1$ with DNA being differently solvated compared to organic solvents. Since there is almost no change in solvation associated with it, it closely resembles the initial $MLCT^1$ formed in water.

5. Conclusions

We find that TR^3 spectroscopy provides unique and valuable information about the nature of $[Ru(phen)_2dppz]Cl_2$ excited states which complements transient absorption, anisotropy and luminescence studies. Taken together, we propose a model for the complex in isotropic fluids where excitation produces MLCT to all ligands ('precursor' state) which is rapidly (<1 ps) equilibrated as a result of inertial solvent response. This is followed by slower ILET to the dppz ligand which is coupled to diffusive solvent reorganisation, and possibly also counterion reorganisation. In line with previous proposals, the state thus formed ($MLCT^1$) is emissive in organic solvents but converts to another non-emissive state ($MLCT^2$) in water. In DNA, it appears that the anisotropy of the environment which places dppz in a very different environment to the ancillary phen ligands results in the excited state being very rapidly localised on the dppz ligand so that only local relaxation of $MLCT^1$ is observed.

[4] A lifetime of ~5 ps has been reported for establishment of the lowest excited state of $[Ru(bpy)_3]^{2+}$ in acetonitrile under certain pump-probe conditions [42], but with other conditions only faster processes (100–300 ps) were observed [41,43].

6. Abbreviations

bpy	2,2′-bipyridine
$C4(cpdppz)_2$	*N,N′*-bis(cpdppz)-1,4-diaminobutane
cpdppz	12-cyano-12,13-dihydro-11*H*-8-cyclopenta[*b*]dipyrido[3,2-*h*:2′,3′-*j*]phenazine-12-carbonyl
cpdppzOMe	12-cyano-12,13-dihydro-11*H*-8-cyclopenta[*b*]dipyrido[3,2-*h*:2′,3′-*j*]phenazine-12-carboxylic acid methyl ester
CT-DNA	calf-thymus DNA
dppz	dipyrido[3,2-*a*:2′,3′-*c*]phenazine
FWHM	full width at half maximum
ILET	interligand electron transfer
MLCT	metal to ligand charge transfer
phen	1,10-phenanthroline
P/*Ru*	DNA to ligand ratio where *P* is the concentration of DNA phosphate groups (=DNA bases) and *Ru* is the concentration of $Ru(phen)_2dppz$ subunits. Saturation of DNA binding occurs at $P/D=4$ for all three compounds used
ΔOD	difference in optical density between the excited state and ground state spectra

Acknowledgements

We are grateful for funding to use the Central Laser Facility at RAL under the EU TMR Large Scale Facility Access Programme (ERBFMGECT9500053). The Swedish Natural Science Research Council (NFR) has also provided funding for this work.

References

[1] B. Norden, P. Lincoln, B. Åkerman, E. Tuite, in: H. Sigel, A. Sigel (Eds.), Metal Ions in Biological Systems, Vol. 33, Marcel Dekker, New York, 1996, pp. 177–252.
[2] E. Amouyal, A. Homsi, J.-C. Chambron, J.-P. Sauvage, Dalton Trans. (1990) 1841–1845.
[3] J.-C. Chambron, J.-P. Sauvage, Chem. Phys. Lett 182 (1991) 603–607.
[4] R.B. Nair, B.M. Cullum, C.J. Murphy, Inorg. Chem. 36 (1997) 962–965.
[5] V.W.-W. Yam, K.K.-W. Lo, K.K. Cheung, R.Y.-C. Kong, Chem. Commun. (1995) 1191–1192.
[6] H.D. Stoeffler, N.B. Thornton, S.L. Temkin, K.S. Schanze, J. Am. Chem. Soc. 117 (1995) 7119–7128.
[7] E. Sabatini, H.D. Nikol, H.B. Gray, F.C. Anson, J. Am. Chem. Soc. 118 (1996) 1158–1163.

[8] X.-Q. Guo, F.N. Castelano, L. Li, J.R. Lakowicz, Biophys. Chem. 71 (1998) 51–62.
[9] A.E. Friedman, J.-C. Chambron, J.-P. Sauvage, N.J. Turro, J.K. Barton, J. Am. Chem. Soc. 112 (1990) 4960–4962.
[10] C. Hiort, P. Lincoln, B. Norden, J. Am. Chem. Soc. 115 (1993) 3448–3454.
[11] Y. Jenkins, A.E. Friedman, N.J. Turro, J.K. Barton, Biochemistry 31 (1992) 10809–10816.
[12] E. Tuite, P. Lincoln, B. Nordén, J. Am. Chem. Soc. 119 (1997) 239–240.
[13] J.-C. Chambron, J.-P. Sauvage, E. Amouyal, P. Koffi, New J. Chem. 9 (1985) 527–529.
[14] C. Turro, S.H. Bossmann, Y. Jenkins, J.K. Barton, N.J. Turro, J. Am. Chem. Soc. 117 (1995) 9026–9032.
[15] E.J.C. Olsen, D. Hu, A. Hörmann, A.M. Jonkman, M.R. Arkin, E.D.A. Stemp, J.K. Barton, P.F. Barbara, J. Am. Chem. Soc. 119 (1997) 11458–11467.
[16] B. Önfelt, P. Lincoln, B. Nordén, J.S. Baskin, A.H. Zewail, Proc. Natl. Acad. Sci. USA 97 (2000) 5708–5713.
[17] M.N. Ackermann, L.V. Interrante, Inorg. Chem. 23 (1984) 3904–3911.
[18] J. Fees, W. Kaim, M. Moscherosch, W. Matheis, J. Klíma, M. Krejcik, S. Zális, Inorg. Chem. 32 (1993) 166–174.
[19] J. Fees, M. Ketterle, A. Klein, J. Fielder, W. Kaim, Dalton Trans. (1999) 2595–2599.
[20] C.G. Coates, L. Jacquet, J.J. McGarvey, S.E.J. Bell, A.H.R. Al-Obaidi, J.M. Kelly, J. Am. Chem. Soc. 119 (1997) 7130–7136.
[21] D. Bates, Preparation, Characterization, and Photophysical Investigation of Polypyridyl Re(I), Ru(II), and Os(II) Complexes, PhD thesis, University of North Carolina, 1994.
[22] C.G. Coates, P.L. Callaghan, J.J. McGarvey, J.M. Kelly, P.E. Kruger, M.E. Higgins, J. Raman Spectrosc. 31 (2000) 283–288.
[23] S. Waterson, H.J. Bakker, Nature 402 (1999) 506–507.
[24] A.C. Benniston, P. Matousek, A.W. Parker, J. Raman Spectrosc. 31 (2000) 503–507.
[25] P. Matousek, M. Towrie, C. Ma, W.M. Kwok, D. Phillips, W.T. Toner, A.W. Parker, J. Raman Spectrosc. 32 (2001) 983–988.
[26] B. Önfelt, P. Lincoln, B. Norden, J. Am. Chem. Soc. 121 (1999) 10846–10847.
[27] B. Önfelt, P. Lincoln, B. Norden, J. Am. Chem. Soc. 123 (2001) 3630–3637.
[28] M. Towrie, A.W. Parker, W. Shaikh, P. Matousek, Meas. Sci. Technol. 9 (1998) 816.
[29] R.B. Nair, E.S. Teng, S.L. Kirkland, C.J. Murphy, Inorg. Chem. 37 (1998) 139–141.
[30] R.B. Nair, L.K. Yeung, C.J. Murphy, Inorg. Chem. 38 (1999) 2536–2538.
[31] C.E. Keller, C. Pollard, L.K. Yeung, W.D. Plessinger, C.J. Murphy, Inorg. Chim. Acta 298 (2000) 209–215.
[32] C.G. Coates, J. Olofsson, N. Colletti, J.J. McGarvey, B. Önfelt, P. Lincoln, B. Norden, E. Tuite, P. Matousek, A.W. Parker, J. Phys. Chem. B 105 (2001) 12653–12664.
[33] C.G. Coates, P. Callaghan, J.J. McGarvey, J.M. Kelly, L. Jacquet, A. Kirsch-De Mesmaeker, J. Mol. Struct. 598 (2001) 15–25.
[34] K. Nozaki, K. Miyawaki, T. Ohno, XVIII IUPAC Symposium on Photochemistry, Dresden, 2000, Book of Abstracts, p. 470.
[35] C. Rønne, P.-O. Åstrand, S.R. Keiding, Phys. Rev. Lett. 8 (1999) 2888–2891.
[36] J. van Houten, R.J. Watts, J. Am. Chem. Soc. 97 (1975) 3843–3844.
[37] M.L. Horng, J.A. Gardecki, A. Papazyan, M. Maroncelli, J. Phys. Chem. 99 (1995) 17311–17337.
[38] J. Ferguson, E. Krausz, Inorg. Chem. 25 (1986) 3333–3335.
[39] J. Ferguson, E. Krausz, M. Maeder, J. Phys. Chem. 89 (1985) 1852–1854.
[40] T. Yabe, L.K. Orman, D.R. Anderson, S.-C. Yu, X. Xu, J.B. Hopkins, J. Phys. Chem. 94 (1990) 7128–7132.
[41] L.F. Cooley, P. Bergquist, D.F. Kelley, J. Am. Chem. Soc. 112 (1990) 2612–2617.
[42] R.A. Malone, D.F. Kelley, J. Chem. Phys. 95 (1991) 8970–8976.
[43] N.H. Damrauer, G. Cerullo, A. Yeh, T.R. Boussie, C.V. Shank, J.K. McCusker, Science 275 (1997) 54–57.
[44] N. Damrauer, J.K. McCusker, J. Phys. Chem. A 103 (1999) 8440–8446.
[45] A.T. Yeh, C.V. Shank, J.K. McCusker, Science 289 (2000) 935–938.
[46] P. Lincoln, A. Broo, B. Norden, J. Am. Chem. Soc. 118 (1996) 2644–2653.